PARTIAL SAFETY FACTORS FOR PRESTRESSED CONCRETE GIRDERS STRENGTHENED WITH CFRP LAMINATES

D. Dias-da-Costa[1], L.A.C. Neves[2], S. Gomes[3], R. Graça-e-Costa[4], S.A. Hadigheh[5], P. Fernandes[6]

[1]Associate Professor, School of Civil Engineering, Univ. of Sydney, Sydney, NSW 2006, Australia; Institute for Sustainability and Innovation in Structural Engineering, Dept. of Civil Engineering, Univ. of Coimbra, Rua Luís Reis Santos, Coimbra 3030–788, Portugal (corresponding author). Email: daniel.diasdacosta@sydney.edu.au

[2] Assistant Professor, Resilience Engineering Research Group, University of Nottingham, Faculty of Engineering, University Park, United Kingdom.

[3]Researcher, ISISE, Department of Civil Engineering, University of Coimbra, Rua Luís Reis Santos, 3030–788 Coimbra, Portugal.

[4]Assistant Professor, CEPAC, Universidade do Algarve, Campus de Gambelas, 8005-139 Faro, Portugal; CEris-ICIST, DECivil, Instituto Superior Técnico, Universidade de Lisboa, Av. Rovisco Pais, 1049-001 Lisboa, Portugal.

[5]Lecturer, School of Civil Engineering, The University of Sydney, Sydney, NSW 2006, Australia.

[6]Associate Professor, Civil Engineering Department, Instituto Politécnico de Leiria, Portugal; CEris-ICIST, DECivil, Instituto Superior Técnico, Universidade de Lisboa, Av. Rovisco Pais, 1049-001 Lisboa, Portugal.

Abstract

This paper provides a framework for the calibration of partial safety factors in prestressed concrete (PC) girders strengthened in flexure with carbon fibre-reinforced polymer (CFRP) laminates. A hybrid approach was proposed to take advantage of comprehensive non-linear numerical models in reliability analysis using a first order reliability method (FORM) in conjunction to the response surface method (RSM). The PC girders selected for analyses were taken from real structures designed and built since the 1980s, based on old standards, now requiring strengthening and upgrade due to partial corrosion of prestressing strands. Using the proposed approach, a sensitivity analysis was performed to identify the most relevant variables and assess the area of CFRP laminates needed to restore the capacity to new design standards. Following this study, a partial safety factor was proposed for strengthening PC girders using CFRP laminates. A sensitivity analysis also showed the traffic loads and model uncertainties to be the most important variables for calibration.

Keywords: CFRP laminates; concrete girder; reliability; numerical models; partial safety factors; target reliability index.

Introduction

Many reinforced concrete (RC) bridges built in the last decades using precast prestressed concrete (PC) girders are currently in need of retrofit or upgrade due to degradation and increasing traffic. As interventions are progressively undertaken, the use of externally bonded fibre-reinforced polymer (EB FRP) laminates is a competitive technique when compared with other options (e.g., concrete jacketing or epoxy-bonded steel plates). This is due to the low weight and thickness of FRP laminates, easy application, high stiffness and strength, corrosion protection and reasonable costs (CEB-FIB 2001).

There are currently several guidelines applicable to EB FRP laminates, such as the CEB-FIB (2001), ACI 440.2R-08 (2008), CNR (2001), TR-55 (2000), and the AS 5100.8 (2017). To design strengthening solutions using FRP laminates, the guidelines adopt a limit state approach, where safety or reduction factors, respectively, γ_f and ϕ_f, are either applied to the overall resistance or to each material property, depending on the standard. A summary of these factors for carbon FRP (CFRP) laminates is shown in Table 1.

Despite the standards available, there are still limitations in terms of their scope of application. Specifically, the partial safety factors were mostly developed for new construction and may not directly apply to rehabilitation/strengthening of existing structures. In this case, the assessment of the partial safety factor to be adopted certainly depends on the type of structure and loading conditions such as flexural, on the confinement (Baji 2017), on the standard adopted in the original design, current state of damage, as well as, on the new standard in place when rehabilitation is sought. In the European context, for example, this issue is particularly critical given that many structures were designed using former national guidelines, which are often less demanding than the new guidelines now in use by all partner countries.

Several researchers (Coelho et al. 2018; El-Tawil and Okeil 2002; Monti and Santini 2002; Okeil et al. 2002; Plevris et al. 1995) addressed the uncertainties in the quantification of safety factors applicable to structures strengthened in flexure with FRP laminates. The general approach is based on the creation of a database with a wide range of parameters and Monte Carlo simulations for each designed member. The resulting randomly generated data sets are then used to develop a resistance model for strength. The probability of failure and the reliability index are normally assessed using a first order reliability method (FORM) with the subsequent calibration of flexural resistance factors. One of the first studies in this scope was carried out by Plevris et al. (1995) focusing on reinforced concrete beams strengthened with CFRP laminates. The authors classified the strength and the ultimate strain of the concrete and area of the CFRP laminates as most relevant properties, and calibrated safety factors for a target reliability index of 3.0. It should be mentioned that this study did not include structural rehabilitation. This was addressed later in the studies from Okeil et al. (2002), and El-Tawil and Okeil (2002), where CFRP laminates were used to restore the capacity of degraded bridge girders. The strength reduction factors were calibrated for target reliability index factors of around 3.75. Atadero and Karbhari (2008) performed a reliability study on RC T-beams strengthened with CFRP laminates using real design situations. They developed a methodology to calibrate the strength factors for flexural strengthening based on three reliability indices (2.5, 3.0 and 3.5). They used a simplified analytical model for the debonding of CFRP laminates and showed the reliability of beams to strongly depend on the amount of reinforcement that remains uncorroded in the damaged structure. Intermediate crack and end debonding failure modes on FRP-retrofitted RC T-beams were considered by Pham and Al-Mahaidi (2008). Their study found that the type of debonding significantly decreases reduction factors in the reliability analysis.

It is quite common to perform reliability studies using simplified analytical models with a common assumption of perfect bond between FRP and substrate. In fact, limited research has considered intermediate crack debonding – even if this effect is critical in the analysis of safety factors (Pham and Al-Mahaidi 2008). It is not yet known to which extent the underlying simplifications are safe for design. For example, the interaction of cracks and the debonding, or the failure of the FRP laminates, all are highly related phenomena, and their consideration in numerical models could potentially lead to more demanding safety/reduction factors based on reliability analyses. The study presented in this paper contributes towards these research questions by focusing on the reliability analysis of PC bridge girders strengthened in flexure with CFRP laminates.

The girders selected for analysis are taken from existing PC bridges requiring strengthening based on a set of idealised damage due to corrosion of prestressing steel. The girders were originally designed and built since the 1980s using old standards, in which case any strengthening solution sought here – attachment of CFRP laminates– needs to comply with new standards, in this case European Standards EN1991-2 (2002) and EN1992-2 (2005). The paper quantifies the partial safety factors that could be used for designing the strengthening solution with CFRP laminates and presents a new hybrid procedure to take advantage of non-linear FEM models to accurately simulate the material and structural behaviour thus obtaining a more refined solution in reliability analysis.

The proposed hybrid method combines an analytical simplified model to obtain a first estimate on the reliability index, after which an advanced FEM model searches for a more refined solution for designing the strengthened structure. The study also focusses on the requirements created by the replacement of old standards by the Eurocodes, since these are often significantly more demanding in terms of safety and loads. Up to the authors knowledge, the study presented in this paper is the first that directly proposes a hybrid method for reliability analysis and quantifies partial safety factors for damaged prestressed concrete girders strengthened with bonded CFRP laminates in the scope of the Eurocodes. The new framework is quite general and can be easily adapted to other codes.

Design cases

The bridges studied in this paper are based on a simply-supported structural scheme widely used in main roads connecting mid-sized towns in Portugal. The span is relatively short when compared with most recent practice in construction and ranges between 13 and 19 m. The bridge was designed for one traffic lane in each direction, with a side-walk on both sides. The structure was composed of three prestressed concrete 'I'-shaped girders – see cross-section defined in Figure 1 and dimensions in Table 2. The mean concrete compressive strength, f_{cm}, was 43 MPa, the mean tensile strength, f_{ctm}, was 3.2 MPa and the mean Young's modulus, E_{cm}, was 34 GPa. Please note that the notation adopted is in accordance with Eurocode 2 EN1992-2 (2005).

The bridges complied with the provisions from REBAP (1983) with design loads given in RSA (1983). It is worth mentioning that both ultimate and service limit states were considered in the original design. The exterior girder is typically the most critical and is herein considered for further analyses. The three representative spans adopted are, 13 m, 16 m and 19 m, in which case the corresponding main dimensions of the exterior girder are summarised in Table 2.

It should be mentioned that the design loads required by the new European Standards EN1991-2 (2002) and EN1992-2 (2005) can be significantly higher than those obtained with the old standard. For example, the ratio between live and dead bending moments for the shortest span reaches a factor of 3 in the new standard, whereas the same factor drops to 2 in the old one. This means that upgrading the girder also requires strengthening to meet the new standard. The unstrengthened (or undamaged) situation is the reference (D0) in the study that follows. In addition, six damaged scenarios are chosen for the same girder caused by corrosion of prestressing strands. Such scenarios are defined by assuming the loss of area for the prestressing strands ranging from 10 to 30% affecting one (Dx) or the two (2Dx) levels of reinforcement. A summary of all scenarios and the remaining (i.e. uncorroded) area of the prestressing strands, A_p, is given in Table 3.

The strengthening of the PC girders is to be achieved using CFRP laminates with anchorage at both ends, as to obtain the maximum benefit from strengthening with CFRP laminates (Garden and Hollaway 1998; Quantrill and Hollaway 1998). The area of the CFRP laminates should restore the structural capacity of the girders.

Proposed hybrid model for reliability analysis

This section proposes a hybrid model for reliability analysis using the design cases defined in the previous section, with the purpose of determining the design area of CFRP laminates to comply with the reliability index as defined by EN 1990 (2002).

General background

Failure is herein defined as the random structural resistance, *R*, being lower than the current random load demand, *S*, in which case (Bucher 2009; FERUM 2010; Melchers 2017):

$$P_f = P\left(R - S < 0\right), \tag{1}$$

and structural reliability is defined by $1 - P_f$, which identifies the probability of the structure performing its intended function. The relationship $R - S$ is designated by limit state function and is a boundary separating acceptable and unacceptable structural performance depending on the random variables defined. Graphically, the probability of failure corresponds to the grey volume represented in Figure 2.a if only two variables are considered.

The reliability index, β, and the probability of failure, can both be shown to be equivalent. Geometrically, the former parameter directly measures the minimum distance from the origin to the failure domain. This point is the so-called design point – see representation in Figure 2.b $\left(r^*, s^*\right)$ – and its cosines direction measure the importance of each parameter on the probability of failure, where a positive value means that an increase of the mean value also increases safety (see Figure 2.c).

The limit state function is typically defined using several variables that may not be normally distributed. In this case, the random variables are transformed from the original space to a standard normal space, which simplifies calculations since the transformed variables will follow an approximated normalised distribution. This normalisation can be applied using the Nataf transformation described by Melchers (2017). It should be mentioned that there is not usually a closed-form equation available for the limit state function. Therefore, the derivation of the reliability index requires an iterative approach to identify the design point. FORM uses a Taylor expansion in the neighbourhood of the design point that is progressively refined. For highly non-linear problems, however, a combination of FORM with the response surface method (RSM) can be more effective. The RSM is used to approximate the non-linear limit state function by a regression function of lower-order polynomials (Bucher, 2009) using selected support points for each random variable. The reliability index is then determined within two iterative cycles, the first uses RSM to compute an approximated limit state function, and the second applies FORM to determine the reliability index for the approximated limit state function. Both are applied sequentially until converging into a design point within an acceptable threshold.

In the following section, a new methodology is proposed for the efficient use of RSM and FORM with advanced non-linear numerical models for prestressed concrete girders strengthened with CFRP laminates. The methodology combines both analytical and numerical models to limit the use of time-consuming calculations in the search for the design point.

Methodology implemented

The limit state function, G, was herein defined by the difference between the resistance and standardised traffic loads, as follows:

$$G = \gamma_{mtl} - \gamma_{tl}, \qquad 2$$

where γ_{mtl} is the maximum traffic load scale factor supported by the girder – obtained using the analytical and FEM models as described ahead – and γ_{tl} is the traffic load scale factor. The model uncertainties are considered as:

$$G = \gamma_{mtl}(\theta_E) \times \theta_R - \gamma_{tl}, \qquad 3$$

where θ_R is the resistance model uncertainty and θ_E is the load model uncertainty. The resistance uncertainty is directly multiplied by the scale factor, whereas the load uncertainty is assigned to the structural model to affect both traffic and remaining loads.

The maximum traffic scale factor is obtained from the ultimate load, and is a function of all remaining random variables, including dead loads. Therefore, the limit state function can be written as:

$$G = \gamma_{mtl}(\theta_E; \nu_1; \nu_2; \nu_3; \ldots; \nu_n) \times \theta_R - \gamma_{tl}, \qquad 4$$

where ν_i stands for the random variables.

A hybrid process is herein proposed using RSM and FORM to efficiently take advantage of comprehensive non-linear numerical models. For this purpose, analytical and numerical models are progressively used in the analysis to calculate the area of laminates needed for strengthening the structure and reach the necessary target index. This parameter is taken from EN 1990 (2002) for a level of high economic, social and environmental consequences for structural failure, in which case β_t is 4.3. Please note that more details about each model are provided ahead.

The analytical model is used to calculate the area of the strengthening laminate, A_f, corresponding to the target reliability index defined in the standard. The area of the laminate is searched incrementally, so that each step starts by guessing the area and then obtaining the reliability index using RSM and FORM. If this index is within 1% error of the target, the non-linear numerical model is engaged in a second stage of analysis leading to a more accurate search. This procedure is very efficient, since the use of a computationally demanding non-linear model is minimal and only applied to fine-tune the final reliability index.

Within each cycle of analysis, the iterative procedure first calculates the reliability index, as represented in Figure 3. This is carried out by initialising the design points, dp_0, and reliability index, β_0, with mean values used for the random variables. RSM is then applied to define the response surface in the neighbourhood of the design and support points. Analytical and numerical models are used to run structural analyses and define the response surfaces. Finally, a new estimate for the design points, d_{n+1}, is obtained from FORM by calculating the maximum load scale factor at the design point, dp_n, including an updated reliability index, β_{n+1}. If the change in the reliability index is less than 1% the procedure stops and convergence is found. Otherwise, a new surface approximation is calculated with RSM based on the most recent approximation for the design points and the whole cycle starts.

Probabilistic models

Only the most significant variables are herein considered random following the recommendations found in (Gomes et al. 2014). These are the steel strand strength, f_p, CFRP laminates strength, f_t, and resistance model uncertainties, θ_R, on the side of the resistance models, and traffic loads scale factor, γ_{tl}, dead loads, γ_{dl}, self-weight of concrete, γ_c, and load model uncertainties, θ_E, on the side of the load model. Table 4 summarises the statistical descriptions for the adopted variables.

In the definition of the distribution types and coefficients of variation (COV) for each variable, available bibliography was considered. The steel strand strength model was selected based on the study from Jacinto et al. (2012). The CFRP laminates strength model was defined after a probabilistic study by Gomes et al. (2018), where the Weibull distribution was shown to be accurate for probabilistic analyses. The dead loads corresponding to the weight of sidewalks, guard rails and asphalt are considered uniformly distributed over the girder, following a normal distribution with a COV of 0.10 (von Scholten and Vejdirektoratet 2004).

The statistic values of the traffic loads, Q, can be assumed to have a normal distribution according to von Scholten and Vejdirektoratet (2004). Considering that the nominal values defined in the standard correspond to the 95 th percentile and that the bridge lifetime horizon is 50 years for the strengthened situation, the distribution for the maximum load asymptotically approaches a Gumbel distribution with mean and standard deviation values (Ang and Tang 2007) provided by the following:

$$\mu = u_n + \frac{\gamma}{\alpha_n} \tag{5}$$

$$\sigma = \frac{\pi}{\sqrt{6}\alpha_n} \tag{6}$$

where γ is the Euler–Mascheroni constant (0.5772), n is the time in years, u_n is the shape parameter and α_n is the scale parameter.

The characteristic value of traffic loads from Gumbel distribution is found using the following equation:

$$Q_k = \frac{\mu_{tl}}{1+1.866V_{tl}}, \tag{7}$$

where μ_{tl} and V_{tl} are respectively the mean and the coefficient of variation (COV) of the traffic loads, Q. The 95 th percentile loads scale factor is herein taken as 1 and the COV 0.15 (Atadero and Karbhari 2008; El-Tawil and Okeil 2002; Wisniewski 2007).

The model uncertainties were defined following the range of recommendations in (El-Tawil and Okeil 2002; JCSS 2001), with a mean value of 1.05 and COV of 0.105.

It should be mentioned that effects of the ageing of the epoxy and fatigue loads were not considered in the analyses.

Structural analysis

This section briefly describes the two approaches used for performing the structural analysis of the girders.

- Analytical model

The analytical model is based on a cross-sectional analysis using the stress-strain diagram shown in Figure 4 for a linear strain distribution over the girder depth. Plane sections were assumed to remain plane after bending, in which case the flexural moment is computed as follows:

$$M = F_c z_c + F_p z_p + F_f z_{fu} \tag{8}$$

where F_c is the compressive force in concrete, z_c is the distance from the neutral axis to the upper fibre, x, to the concrete force, F_p is the force due to prestressing strands, z_p is the distance between the prestressing strands and the neutral axis, F_f is the force due to CFRP laminates, and z_f is the distance from the CFRP laminates to the neutral axis.

The constitutive model for concrete under compression is modelled using the stress-strain relation given in EN 1992-1-1 (2004):

$$\frac{\sigma_c}{f_c} = \frac{k\eta - \eta^2}{1 + (k-2)\eta}, \tag{9}$$

with

$$\eta = \frac{\varepsilon_c}{\varepsilon_{c1}} \text{ and } k = 1.05 E_c \frac{|\varepsilon_{c1}|}{f_c} \tag{10}$$

where ε_{c1} is the strain at peak stress according to EN 1992-1-1 (2004), E_c is the secant Young's modulus of concrete, and f_c is the concrete cylinder compressive strength. The tensile strength of concrete is disregarded in the analysis.

The ultimate strength of the cross-section is calculated in two main stages of analysis. In the first stage, the stress state at the cross-section is calculated before strengthening, so that the stress/strains installed just before applying the CFRP laminates are known. This first step is critical to assess the initial strain at the soffit of the girder, where CFRP laminates are going to be applied, and that will no longer be transferred to the laminates once the strengthening system is fully operational. In the second stage of analysis, the ultimate moment of the girder is finally obtained by identifying which failure mode occurs first, i.e. the mode with the lowest bending moment. All possible situations are accounted for, e.g. debonding and failure at CFRP laminates, crushing of concrete, prestressing strands reaching the 0.1% proof stress before (or simultaneously) with failure at CFRP laminates. During each stage of analysis all calculations are performed following a standard iterative procedure that searches for the location of the neutral axis and assures the balance of forces inside the cross-section.

- Numerical model

A finite element model based on the discrete strong discontinuity approach (DSDA) is used to perform the advanced analysis of the structural behaviour of the concrete girders strengthened with

CFRP laminates (Dias-da-Costa et al. 2018b). The model is based on finite elements enhanced by additional degrees of freedom that are progressively placed along the crack paths to measure their widths. The effect of the crack opening is then transmitted to the edges of the enhanced element as a rigid body movement that increases the overall deformability of the structure due to damage propagation and development (see Figure 5a). During the structural analysis, new cracks are activated inside each element whenever the strength of concrete is reached, therefore preventing the maximum tensile stress to rise above it. Each crack undergoes a traction-separation law that softens the tensile stress, simultaneously reducing the stiffness of the element while increasing the crack width. The development of the model from a conceptual and mathematical points of view can be found in (Dias-da-Costa et. al 2009).

The embedded cracks can naturally interact with steel and strengthening material, thus capturing the local debonding and increased deformation due to damage of the materials. This capability is critical to accurately predict the ultimate strength of the member (Dias-da-Costa et al. 2018b). Figure 5b compares a discrete crack model with smeared models in the neighbourhood of highly-localised stress fields caused by the opening of a crack and represents the local stretching and failure of the CFRP laminates. Such model was shown to provide reliable results in terms of crack propagation, crack patterns and crack openings for both service and ultimate loads in concrete members under flexural loads (Dias-da-Costa et al. 2010; 2017 and 2018aa). A detailed presentation about the implementation aspects can be found in (Dias-da-Costa et al. 2009; 2013 and 2013).

The numerical model is validated using experimental data from flexural tests performed on PC girders, one with and two without CFRP laminates (Fernandes 2007; Fernandes et al. 2013) – see Figure 6a. The 'I'-shaped girders were tested under flexural loading. The active reinforcement was composed by twelve 3/8" prestressing bonded strands at bottom and two 3/8" unbonded post-tensioning strands at the top of the cross-section – see Figure 6b. The stirrups in the web were 5 mm bars with 500 MPa yield stress in a two-legged arrangement with 150 mm spacing along the span. The pre-tensioning strands were initially stretched to 1,430 MPa before pouring concrete and kept attached to the precast table, i.e., not engaged with the girder until day 5. At that age, six pre-tensioning strands were released and the post-tensioning strands were stretched to 1,160 MPa. Next, the six remaining pre-tensioning strands were cut from the table and the girder fully demoulded. The post-tensioning strands were only installed to avoid premature failure due to the high level of stress applied by the pre-tensioning strands at such an early age. It should be highlighted that once the girders are finally taken to the construction site to erect the bridge, the post-tensioning strands are meant to be deactivated after enough vertical load is applied to the structure. These girders were part of a linkage project with precast industry to study the economical and practical possibility of extremely short turnaround times, in which case high-strength concrete was used to allow enough compressive strength when releasing the pre-tensioning strands at an early age. The girders were designed and experimentally tested by one of the co-authors and were selected for validation of the numerical model given that very detailed information was available. The properties for the high-strength concrete were experimentally characterised and are listed in Table 5. The strengthening of the girder was also addressed by the original experimental programme. The CFRP laminates used in the strengthened girder consisted of two CFK 150/2000 with rectangular cross-section of 100×1.4 mm^2 anchored at the extremities. Figure 7 shows the failure after the tests.

The numerical simulations are based on 2D analysis using the finite element mesh shown in Figure 8. Plane stress bilinear (i.e. 4-node) elements are adopted for simulating concrete, whereas linear truss (i.e. 2-node) elements are used for simulating steel reinforcements and CFRP laminates. Since the CFRP laminates are very thin, their bending is negligible compared to the axial component. This makes it particularly suitable for simulation using 2-node elements showing only axial stiffness, i.e., standard truss elements – these are also used for modelling the strands and stirrups. The truss elements are connected to the concrete elements using zero-thickness interface elements, which directly follow the bond-slip law of the CFRP laminates. Further details can be found in (Dias-da-Costa et al. 2018b), where focus was given to the modelling of concrete slabs strengthened with CFRP laminates and its interaction with fracture. Interface elements are also adopted to model the bond behaviour of the prestressed strands. The stirrups are modelled using the 2-node truss elements directly connected to the concrete elements with 150 mm along the beam with the area of the two-legged arrangement described earlier. Given that the stress state in the girder is mostly bidimensional for the structural and loading schemes adopted, this assures that the confinement provided by the stirrups and resistance against shear are adequately approximated.

The concrete is assumed elastoplastic under compression as defined in EN 1992-1-1 (2004). For tension, embedded cracks are used to capture the non-linear effect using a bilinear softening law with the fracture energy defined by CEB-FIP Model Code 1990 (1991). The prestressing strands and stirrups are modelled considering the bilinear law defined in EN 1992-1-1 (2004) with the parameters shown in Table 5, whereas the CFRP laminates are modelled with a linear elastic behaviour. Perfect bond conditions are assumed between concrete and reinforcements, whereas the bond between CFRP laminates and concrete is modelled using the simplified model proposed by Lu et al. (2005) – see Appendix A for more details. The *automatic* method proposed by Graça-e-Costa et al. (2013) is used to overcome convergence issues during the stages of concrete cracking and crushing, yielding of steel reinforcements, and local debonding at CFRP laminates-concrete interfaces (Graça-e-Costa et al 2012; 2013).

It should be mentioned that two different procedures can be usually followed to simulate the forces due to the pre-tensioning strands. The first option consists in applying a negative uniform temperature variation to the pre-tensioning strands at day 5 corresponding to the opposite stretch that was applied to the strands before casting, i.e. corresponding to 1,430 MPa. The second option available – which was the one followed in this paper – directly applies the compressive force caused by the pre-tensioning strand to the girder. These stresses are the same that appear when the pre-tensioning strand is finally cut from the precast table. The initial tensile strain/stress in the pre-tensioning strands is stored and considered when computing the total tensile stress at the strand. Naturally, the tensile stress of the strand obtained just after releasing is lower than 1,430MPa, both numerically and experimentally, due to the bending and axial shortening of the girder caused by compressive forces. Figure 8 represents all forces applied to the girder – external load F and internal forces P_1, P_2 and P_3 due to the strands. All material parameters adopted in the validation simulations are summarised in Table 5.

Figure 9 shows a comparison between experimental and numerical results for both strengthened and non-strengthened girders. The main stages related with the onset of cracking, the yielding of prestressed reinforcement and concrete crushing are also represented. In summary, a good agreement is observed between numerical and experimental data. In summary, a good agreement is observed between numerical and experimental data. It should be mentioned that even though the numerical model can simulate the global debonding of CFRP laminates accurately – see (Dias-da-Costa et al. 2018b) for a detailed validation of the model– this failure mode could not develop due to the material properties of the cross-section and anchorage of the CFRP laminates. Therefore, the strengthened girder fails with crushing of concrete after the yielding of prestressed tendons, thus confirming the experimental findings. The crack pattern at failure is shown in Figure 10 for both strengthened and non-strengthened models.

Results and discussion

Reliability index and prestressing area before strengthening

Figure 11 shows the variation of the reliability index, β, with the area of pre-tensioning steel, A_p, based on RSA (1983) and EN1991-2 (2002) for the girders with strengthening laminates. In both cases, the reliability index increases with the amount of uncorroded prestressing area in the girder. For similar areas, the reliability values based on the former standard are significantly higher than the ones obtained with the latter code, and in some cases this difference can reach more than 200% – e.g.

when the area of pre-tensioning steel is 1,652 mm^2. This difference is mainly related to the more demanding traffic load requirements in the current standard. Reliability is strongly influenced by the amount of prestressing area of the girder (Atadero and Karbhari 2008) and results show that strengthening is required to reach the target reliability index defined in the new standard in all design cases.

A sensitivity plot for both traffic load models is shown in Figure 12. The most influential variable is the traffic load, γ_{tl}, followed by the load and resistance uncertainties, θ_E and θ_R. The dead loads, γ_{dl}, and the concrete self-weight, γ_c, have a reduced influence in general, whereas the steel strand strength, f_p, has a sensitivity factor close to 0.18. Despite the differences in traffic load models and safety requirements, the cosines direction at design point are nearly the same in both standards.

Sensitivity analysis and design point for the strengthened girders

The area of the CFRP laminates calculated according to the procedure described previously is summarised in Table 6. During the analyses, the possibility of the CFRP laminates debonding and fracturing before concrete crushing and/or the yielding of the steel strands is properly accounted for. All design cases require CFRP laminates to reach the target reliability index, with the flexural capacity of the girders increasing up to 74% for the most degraded cases, B13-2D3, to restore the full capacity according to the EN1991-2 (2002). The reference design case, i.e. the undamaged girder, only requires an upgrade of a maximum of 25%, which directly reflects the increment due to the provisions of the current standard.

The relative importance of the seven random variables considered in the reliability study is presented in Figures 13a-c based on the cosines direction at design points in the normalised space. For each random variable, the several scenarios of corroded pre-tensioning strands are considered. The leftmost bar corresponds to the highest area of pre-tensioning steel and the rightmost bar to the lowest. From these charts, it can be observed that traffic loads, γ_{tl}, play a fundamental role in the analysis, being always the most significant variable, in some cases reaching an importance of almost 0.80.

The load uncertainties also have an important weight in the analysis, ranging from 0.40 to 0.60. In respect to the other loads, namely concrete self-weight, γ_c, and dead loads, γ_{dl}, both of them present lower sensitivity factors, usually smaller than 0.15. On the other hand, the resistance parameter showing the highest importance is the resistance uncertainty, θ_R, presenting values around -0.40 for all analyses. The steel strand strength, f_p, shows values of nearly -0.10 for bridges B13 and B19 and can reach -0.20 for bridge B16. The CFRP laminates strength, f_f, exhibits values up to -0.30, assuming greater importance than the steel strand strength in most analyses. This can be related to the loss of pre-tensioning steel.

Table 7 shows the reliability index and design points used for the calibration of CFRP laminates partial safety factors, i.e., the cases for which the area of CFRP laminates leads to values closest to the target reliability index. Reliability indices are slightly higher than the target of 4.3. This occurs because the numerical model is more accurate than the analytical model for simulating the structural behaviour. However, it should be mentioned that the differences are in the order of 6%, meaning that design using simplified models is safe for the calibration of partial safety factors for CFRP.

As expected, the design values in Table 7 show that the resistance variables, f_p, f_f and θ_R are generally lower than the corresponding mean values. The opposite trend is observed in the load variables, γ_c, γ_{dl}, γ_{tl} and θ_E. Traffic loads exhibit the higher deviation from the mean value, which shows the importance they have for the calibration process.

Calculation of partial safety factors

Table 8 presents the partial safety factors calculated for each model based on the characteristic value for the distribution. The partial safety factors obtained for the CFRP laminates have an average of 1.16. This is consistent with the recommendations found in design guides. For instance, for the design of concrete structures using CFRP end anchored laminates, CEB-FIB (2001) recommends the use of a safety factor of 1.20, a value slightly higher than the one found in this paper. CNR (2001) recommends a factor of 1.10 and TR-55 (2000) is more conservative, suggesting a factor of 1.54 for the same type of strengthening.

Conclusions

This paper proposed a new hybrid procedure to perform reliability analyses efficiently combining analytical and advanced non-linear FEM models to overcome the simplifications normally assumed in reliability studies. The framework developed uses a discrete crack model to capture the interaction between concrete cracks and local debonding of CFRP laminates and was applied to calibrate the partial safety factor required for designing the strengthened PC girders.

The PC girders were taken from existing bridges built to connect small cities since the 1980s, with spans ranging from 13 to 19 m, and originally designed with previous standards. Several corrosion damage scenarios were considered when determining the area of CFRP laminates needed to restore the structural capacity to current standards. The following conclusions are highlighted:

- the partial safety factor for designing strengthening of PC girders with CFRP laminates is in the range of 1.16, and was observed not to change significantly with the span;
- the use of advanced non-linear models entails higher accuracy in the simulation of both material and structural behaviour, particularly concerning the interaction of concrete cracking with the local debonding of CFRP laminates. However, given that the differences relatively to simplified analytical models were found to be in the range of 6%, the use of simplified models for future studies targeting code calibration of partial safety factors for CFRP laminates could be sufficient;
- the sensitivity analysis carried out shown the traffic loads and model uncertainties to be the most significant parameters for the calibration process, assuming high values compared with dead load, concrete self-weight and steel strand strength. Thus, it is important to assess the

model uncertainties for further reliability analysis, particularly in the case of more advanced models now widely available.

It is worthwhile mentioning that the methodology presented in this paper is fully general and can easily be adapted to different standards and geometries where the stress-state is predominantly two-dimensional. The generalisation to three-dimensional structures, however, will require the development of discrete crack models with more robust algorithms to be able to reliably track the geometry of crack propagation, and therefore remain more precise than the uncertainty of the input data.

Acknowledgements

S. Gomes acknowledges the financial support of the Portuguese Science and Technology Foundation (FCT) through the Ph.D. grant number SFRH/BD/76345/2011. D. Dias-da-Costa would like to acknowledge the support from the Australian Research Council through its Discovery Early Career Researcher Award (DE150101703) and Linkage grant (LP140100591). This work was also supported by FCT, within ISISE, project UID/ECI/04029/2013.

Data Availability Statement

Some or all data, models, or code generated or used during the study are available from the corresponding author by request.

Appendix A - Adopted bond-slip law

Lu et al. (2005) model, which is adopted as FRP-to-concrete bond-slip law in this paper, is defined by the following equations:

$$\tau = \tau_{max}\sqrt{\frac{s}{s_0}} \text{ if } s \le s_0, \qquad \text{B-1}$$

$$\tau = \tau_{max} e^{-\alpha\left(\frac{s}{s_0}-1\right)} \text{ if } s > s_0, \qquad \text{B-2}$$

with

$$s_0 = 0.0195\beta_w f_t, \qquad \text{B-3}$$

$$\tau_{max} = \alpha_1 \beta_w f_t, \qquad \text{B-4}$$

$$\alpha = \frac{1}{\frac{G_f}{\tau_{max} s_0} - \frac{2}{3}}, \qquad \text{B-5}$$

$$\beta_w = \frac{2.25 - b_f / b_c}{1.25 + b_f / b_c}, \qquad \text{B-6}$$

$$G_f = 0.309\beta_w^{\,2}\sqrt{f_t}, \qquad \text{B-7}$$

where τ_{max} is the maximum local bond stress, s is the local slip, s_0 is the local slip at τ_{max}, f_t is the concrete tensile strength, b_c and b_f are, respectively, the widths of concrete prism and FRP plate, and G_F is the interfacial fracture energy.

References

AASHTO (American Association of State Highway and Transportation Officials). (2012). "*Guide Specifications for Design of Bonded FRP Systems for Repair and Strengthening of Concrete Bridge Elements.*" AASHTO (2012), Washington, DC.

ACI (American Concrete Institute). (2008). "*Guide for the design and construction of externally bonded FRP system for strengthening concrete structures.*" ACI 440.2R-08, Michigan.

Ang, A. and Tang, W. (2007). "*Probability concepts in engineering: Emphasis on applications in civil & environmental engineering*." 2nd Edition, John Wiley & Sons, Chichester.

Atadero, R. A. and Karbhari, V. M. (2008). "Calibration of resistance factors for reliability based design of externally-bonded FRP composites." *Composites Part B: Engineering*, 39(4), 665-79. doi: 10.1016/j.compositesb.2007.06.004.

Baji, H. (2017). "Calibration of the FRP Resistance Reduction Factor for FRP-Confined Reinforced Concrete Building Columns." *Journal of Composites for Construction*, 21(3), 04016107. doi: 10.1016/j.compstruct.2016.07.003.

Bucher, C. (2009). "Computational Analysis of Randomness in Structural Mechanics: Structures and Infrastructures Book Series, volume 3." CRC Press, London.

CEB-FIB (Comité euro-international du béton). (2001). "*Externally bonded FRP reinforcement for RC structures.",* fib Bulletin No. 14, Geneva, Switzerland.

CEB-FIP (Comité euro-international du béton). (1991). "*CEB-FIP Model Code 1990 : Design Code".* Thomas Telford Services Ltd, London.

CEN (European Committee for Standardization). (2002). "*Eurocode 1: Actions on structures- Part 2: Traffic loads on bridges."*, EN1991-2, Brussels.

CEN (European Committee for Standardization). (2005). "*Eurocode 2: Design of concrete structures. Concrete bridges - design and detailing rules."* EN1992-2, Brussels.

CEN (European Committee for Standardization). (2002). "*Eurocode 0: Basis of structural design."* EN 1990, Brussels.

CEN (European Committee for Standardization). (2004). "*Eurocode 2: design of concrete structures, Part 1-1: General rules and rules for buildings."* EN 1992-1-1, Brussels.

CNR. (2001). "*Guide for the design and construction of externally bonded FRP systems for strengthening existing structures."* National Research Council, Advisory Committee on Technical Recommendations for Construction, Rome, Italy.

Coelho, M., Neves, L. and Sena-Cruz, J. (2018). "Designing NSM FRP systems in concrete using partial safety factors." *Composites Part B: Engineering*, 139, 12-23. doi: 10.1016/j.compositesb.2017.11.031.

Dias-da-Costa, D., Alfaiate, J., Sluys, L. J., Areias, P. and Júlio, E. N. B. S. (2013). "An embedded formulation with conforming finite elements to capture strong discontinuities." *International Journal For Numerical Methods In Engineering*, 93(2), 224-44. doi: 10.1002/nme.4393.

Dias-da-Costa, D., Alfaiate, J., Sluys, L. J. and Júlio, E. (2009). "A discrete strong discontinuity approach." *Engineering Fracture Mechanics*, 76(9), 1176-201. doi: 10.1016/j.engfracmech.2009.01.011.

Dias-da-Costa, D., Alfaiate, J., Sluys, L. J. and Júlio, E. N. B. S. (2010). "A comparative study on the modelling of discontinuous fracture by means of enriched nodal and element techniques and interface elements." *International Journal of Fracture*, 161(1), 97-119. doi: 10.1007/s10704-009-9432-6.

Dias-da-Costa, D., Cervenka, V. and Graça-e-Costa, R. (2018a). "Model uncertainty in discrete and smeared crack prediction in RC beams under flexural loads." *Engineering Fracture Mechanics*, 199, 532-43. doi: 10.1016/j.engfracmech.2018.06.006.

Dias-da-Costa, D., Graça-e-Costa, R., Ranzi, G. and Smith, S. T. (2018b). "Assessment of the Behavior of FRP-Strengthened RC Slabs Using a Discrete Crack Model." *Journal of Composites for Construction*, 22(6), 1–14. doi: 10.1061/(ASCE)CC.1943-5614.0000881.

Dias-da-Costa, D., N. F. do Carmo, R. and Graça-e-Costa, R. (2017). "Numerical modeling of concrete beams under serviceability conditions with a discrete crack approach and noniterative solution-finding algorithms." *Structural Concrete*, 18(1), 225-36. doi: 10.1002/suco.201600130.

El-Tawil, S. and Okeil, A. M. (2002). "LRFD flexural provisions for prestressed concrete bridge girders strengthened with carbon fiber-reinforced polymer laminates." *ACI Structural Journal*, 99(2), 181-90.

Fernandes, P. 2007, "Vigas de Grande Vão Prefabricadas em Betão de Alta Resistência Pré-Esforçado [Precast presstressed high-strengt concrete girders with long-span girders]". Ph.D. thesis, Department of Civil Engineering, University of Coimbra.

Fernandes, P., Sena-Cruz, J., Fernandes, C., Silva, P., Dias-da-Costa, D. and Júlio, E. (2013). "Flexural response of HSC girders strengthened with non- and prestressed CFRP laminates." In Proc. FRPRCS-11. Guimarães, Portugal.

FERUM (2010). "*Finite element reliability using matlab.*" http://www.ifma.fr/FERUM.

Garden, H. N. and Hollaway, L. C. (1998). "An experimental study of the failure modes of reinforced concrete beams strengthened with prestressed carbon composite plates." *Composites Part B: Engineering*, 29(4), 411-24. doi: 10.1016/S1359-8368(97)00043-7.

Gomes, S., Dias-da-Costa, D., Neves, L. A. C., Hadigheh, S. A., Fernandes, P. and Júlio, E. (2018). "Probabilistic-based characterisation of the mechanical properties of CFRP laminates." *Construction and Building Materials*, 169, 132-41. doi: 10.1016/j.conbuildmat.2018.02.190.

Gomes, S., Neves, L., Dias-da-Costa, D., Fernandes, P. and Júlio, E. (2014). "Probabilistic Analysis of High Strength Concrete Girders Strengthened with CFRP". *Vulnerability, Uncertainty, and Risk: Quantification, Mitigation, and Management*, 1274–82, United Kingdom. doi: 10.1061/9780784413609.128.

Graça-e-Costa, R., Alfaiate, J., Dias-da-Costa, D., Neto, P. and Sluys, L. J. (2013). "Generalisation of non-iterative methods for the modelling of structures under non-proportional loading." *International Journal of Fracture*, 182(1), 21-38.

Graça-e-Costa, R., Alfaiate, J., Dias-da-Costa, D. and Sluys, L. J. (2012). "A non-iterative approach for the modelling of quasi-brittle materials." *International Journal of Fracture*, 178(1), 281-98. doi: 10.1007/s10704-012-9768-1.

ISIS (2001). "*Strengthening reinforced concrete structures with externally-bonded fibre reinforced polymers",* Design Manual No. 4, ISIS Canada Corporation, The Canadian Network of Centres of Excellence on Intelligent Sensing for Innovative Structures, Winnipeg, Manitoba, Canada.

Jacinto, L., Pipa, M., Neves, L. A. C. and Santos, L. O. (2012). "Probabilistic models for mechanical properties of prestressing strands." *Construction and Building Materials*, 36, 84-9. doi: 10.1016/j.conbuildmat.2012.04.121.

Joint Committee on Structural Safety (JCSS). (2001). "*Probabilistic Model Code.*". 12th Draft < https://www.jcss.byg.dtu.dk/Publications/Probabilistic_Model_Code > (28 Jan 2018)

Japanese Society of Civil Engineers (JSCE). (2001). "*Recommendations for upgrading of concrete structures with use of continuous fiber sheets - Concrete Series No. 41.*", Tokyo, Japan.

Lu, X. Z., Teng, J. G., Ye, L. P. and Jiang, J. J. (2005). "Bond–slip models for FRP sheets/plates bonded to concrete." *Engineering Structures*, 27(6), 920-37. doi: 10.1016/j.engstruct.2005.01.014.

Melchers, R. E. (2017). "*Structural reliability analysis and prediction, 3rd edition*." Wiley.

Ministério da Habitação, Obras Públicas e Transportes. (1983). "*Regulamento de estruturas de betão armado e pré-esforçado [Reinforced and prestressed concrete structures standard].*" REBAP DL no. 349-C/83, Lisbon, Portugal.

Ministério da Habitação, Obras Públicas e Transportes. (1983). "*Regulamento de segurança e acções para estruturas de edifícios e pontes [Buildings and bridges load and safety standard].*" RSA DL no. 235/83 31st May, Lisbon, Portugal.

Monti, G. and Santini, S. (2002). "Reliability-based Calibration of Partial Safety Coefficients for Fiber-Reinforced Plastic." *Journal of Composites for Construction*, 6(3), 162-7. doi: 10.1061/(ASCE)1090-0268(2002)6:3(162).

Okeil, A. M., El-Tawil, S. and Shahawy, M. (2002). "Flexural reliability of reinforced concrete bridge girders strengthened with carbon fiber-reinforced polymer laminates." *Journal of Bridge Engineering*, 7(5), 290-9. doi: 10.1061/(ASCE)1084-0702(2002)7:5(290).

Pham, H. B. and Al-Mahaidi, R. (2008). "Reliability analysis of bridge beams retrofitted with fibre reinforced polymers." *Composite Structures*, 82(2), 177-84. doi: 10.1016/j.compstruct.2006.12.010.

Plevris, N., Triantafillou, T. C. and Veneziano, D. (1995). "Reliability of RC members strengthened with CFRP laminates." *Journal of Structural Engineering*, 121(7), 1037-44. doi: 10.1061/(ASCE)0733-9445(1995)121:7(1037).

Quantrill, R. J. and Hollaway, L. C. (1998). "The flexural rehabilitation of reinforced concrete beams by the use of prestressed advanced composite plates." *Composites Science and Technology*, 58(8), 1259-75. doi: 10.1016/S0266-3538(98)00002-5,

Standards Australia. "*Bridge design- Part 8: Rehabilitation and strengthening of existing bridges.*" AS 5100.8 (2017), Sydney, Australia.

TR-55 (2000). "*Design guidance for strenghening concrete structures using fibre composite materials.*" The Concrete Society, Crowthorne, Berkshire.

Schneider, J. (1997). "*Introduction to safety and reliability of structures.*" International Association for Bridge and Structural Engineering, Zurich, Switzerland.

von Scholten, C. and Vejdirektoratet, D. (2004). "*Reliability-based classification of the load carrying capacity of existing bridges*." The Directorate, Denmark.

Wisniewski, D. F. (2007). "Safety Formats for the Assessment of Concrete Bridges." PhD thesis, Universidade do Minho, Portugal."

Figures caption list

Figure 1. Cross-section and details of the exterior girder (dimensions are in meters if not stated otherwise).

Figure 2. (a) Joint density function $f_{R,S}\left(r,s\right)$ of two random variables with marginal density functions f_r and f_s; (b) Reliability index and design point in the standard space, assuming a linear limit state function and two random variables u_1 and u_2; and (c) cosines direction α at design point u^*. Figure adapted from Schneider (1997).

Figure 3. Flowchart showing both stages of analysis and iterative cycles.

Figure 4. Stress-strain diagram for cross-sectional analysis of PC girders.

Figure 5. (a) Finite elements with embedded cracks. (b) Interaction between FRP and cracks in the scope of discrete and smeared models.

Figure 6. Loading scheme and cross-section of the girder: (a) side view (dimensions in m); and (b) cross-section (dimensions in mm unless stated otherwise).

Figure 7. Tested PC girder: (a) control, and (b) CFRP-strengthened girders.

Figure 8. Mesh used in finite element analysis including loading and boundary conditions.

Figure 9. Load-displacement curves for: (a) non-strengthened; and (b) CFRP-strengthened girders.

Figure 10. Detail of the deformed shape and crack pattern at failure: (a) identification of the detailed region; (b) non-strengthened; and (c) CFRP-strengthened girders. Note: for illustration purpose crack widths are magnified by a factor of 20 and only widths above 0.25 mm are shown.

Figure 11. Reliability index as a function of the area of the pre-tensioning steel in non-strengthened girders according to: (a) RSA (1983); and (b) EN1991-2 (2002)

Figure 12. Cosines direction at design point.

Figure 13. Cosines direction at design point as a function of the pre-tensioning steel (a) B13, (b) B16, and (c) B19.

Table list

Table 1. Summary of safety and reduction factors, respectively γ_f and ϕ_f.

Design guideline	Safety/Reduction factor
CEB-FIB (2001)	γ_f= 1.20 to 1.35
CNR (2001)	γ_f= 1.10 to 1.50
TR-55 (2000)	γ_f= 1.10 to 3.50
JSCE (2001)	γ_f= 1.20 to 1.30
ACI 440.2R-08 (2008)	ϕ_f= 0.85 to 0.95
AASHTO (2012)	ϕ_f= 0.85
ISIS (2001)	ϕ_f= 0.75
AS 5100.8 (2017)	ϕ_f= 0.65 to 0.80

Table 2. Geometry of the bridge girders considered in the study.

Bridge	h	b	b_w	Span (m)
B13	0.6	0.4	0.15	13
B16	0.9	0.6	0.2	16
B19	1.2	0.6	0.2	19

Table 3. Cases of structural deterioration.

Case	% of loss	A_p (mm^2)
D0	0	2,240
D1	10	2,142
D2	20	2,044
D3	30	1,946
2D1	2 × 10	2,044
2D2	2 × 20	1,848
2D3	2 × 30	1,652

Table 4. Statistical properties for the random parameters.

Variable	Mean	Standard deviation	COV	Distribution type
Steel strand strength, f_p (MPa)	1674	50	0.03	Normal
CFRP strength f_t (MPa)	2686	215	0.08	Weibull
Resistance model uncertainties, θ_R	1.0	0.13	0.13	Log-normal
Traffic loads, γ_{tl}	0.78	0.12	0.15	Gumbel
Dead loads, γ_{dl} (kN/m)	10.83	1.08	0.10	Normal
Concrete self-weight, γ_c (kN/m^3)	25.0	1.0	0.04	Normal
Load model uncertainties, θ_E	1.05	0.11	0.10	Log-normal

Table 5. Main material parameters for the validation models.

Parameter		Value
Concrete	Compressive strength	120 MPa
	Tensile strength	5.5 MPa
	Young's modulus	59 GPa
	Fracture energy	0.2 N/mm
Prestressing steel	0.1% proof-stress	1,640 MPa
	Young's modulus	200 GPa
Steel Reinforcement	Tensile strength	500 MPa
	Young's modulus	200 GPa
CFRP	Ultimate strength	2,300 MPa
	Young's modulus	165 GPa

Table 6. Summary of bridges used for calibration.

Bridge	% steel loss	A_p (mm^2)	A_f (mm^2)	Flexural resistance (kNm)	
				Initial	Strengthened
B13	0	2,240	477	2,352	2,902
B13-D1	10	2,142	531	2,239	2,904
B13-D2	20	2,044	586	2,125	2,908
B13-D3	30	1,946	641	2,011	2,914
B13-2D1	2×10	2,044	586	2,135	2,908
B13-2D2	2×20	1,848	688	1,916	2,922
B13-2D3	2×30	1,652	781	1,696	2,945
B16	0	2,240	453	3,336	4,181
B16-D1	10	2,142	508	3,174	4,186
B16-D2	20	2,044	570	3,011	4,194
B16-D3	30	1,946	625	2,849	4,202
B16-2D1	2×10	2,044	563	3,021	4,193
B16-2D2	2×20	1,848	672	2,704	4,213
B16-2D3	2×30	1,652	781	2,385	4,254
B19	0	2,240	445	4,354	5,446
B19-D1	10	2,142	508	4,140	5,453
B19-D2	20	2,044	563	3,926	5,463
B19-D3	30	1,946	625	3,712	5,478
B19-2D1	2×10	2,044	563	3,936	5,441
B19-2D2	2×20	1,848	680	3,518	5,472
B19-2D3	2×30	1,652	789	3,097	5,533

Table 7. Reliability index and design points used for calibration.

Bridge	β	f_p^* MPa	f_f^* MPa	γ_c^* kN/m^3	γ_{dl}^* kN/m	γ_{tl}^*	θ_R^*	θ_E^*
B13	4.36	1,652	2,640	25.4	11.2	1.41	0.78	1.29
B13-D1	4.38	1,666	2,676	25.0	11.2	1.48	0.77	1.25
B13-D2	4.35	1,648	2,539	25.0	10.6	1.42	0.78	1.27
B13-D3	4.41	1,649	2,512	25.3	10.6	1.42	0.78	1.28
B13-2D1	4.32	1,653	2,471	24.9	11.0	1.42	0.78	1.24
B13-2D2	4.33	1,644	2,398	25.1	11.1	1.32	0.80	1.29
B13-2D3	4.34	1,651	2,405	25.1	10.3	1.28	0.80	1.34
B16	4.43	1,649	2,679	25.1	11.3	1.51	0.77	1.23
B16-D1	4.47	1,627	2,585	25.5	11.4	1.30	0.80	1.36
B16-D2	4.57	1,656	2,445	25.3	11.6	1.30	0.80	1.38
B16-D3	4.65	1,615	2,421	24.6	10.6	1.32	0.79	1.35
B16-2D1	4.44	1,628	2,484	25.2	11.0	1.33	0.79	1.33
B16-2D2	4.62	1,672	2,512	25.1	10.8	1.49	0.77	1.27
B16-2D3	4.42	1,641	2,524	25.4	10.8	1.41	0.78	1.29
B19	4.58	1,649	2,752	24.9	11.1	1.48	0.77	1.30
B19-D1	4.45	1,658	2,561	26.0	11.9	1.31	0.80	1.34
B19-D2	4.45	1,657	2,493	25.3	11.7	1.48	0.77	1.21
B19-D3	4.57	1,649	2,492	25.2	10.9	1.38	0.79	1.35
B19-2D1	4.53	1,656	2,568	25.3	11.0	1.42	0.78	1.33
B19-2D2	4.53	1,660	2,513	25.3	11.3	1.42	0.78	1.31
B19-2D3	4.48	1,650	2,521	25.7	10.6	1.47	0.77	1.24

Table 8. Partial safety factors for CFRP.

Bridge	γ_f	Bridge	γ_f	Bridge	γ_f
B13	1.12	B16	1.12	B19	1.09
B13-D1	1.12	B16-D1	1.12	B19-D1	1.13
B13-D2	1.16	B16-D2	1.18	B19-D2	1.20
B13-D3	1.17	B16-D3	1.20	B19-D3	1.18
B13-2D1	1.19	B16-2D1	1.18	B19-2D1	1.15
B13-2D2	1.21	B16-2D2	1.18	B19-2D2	1.18
B13-2D3	1.19	B16-2D3	1.17	B19-2D3	1.18

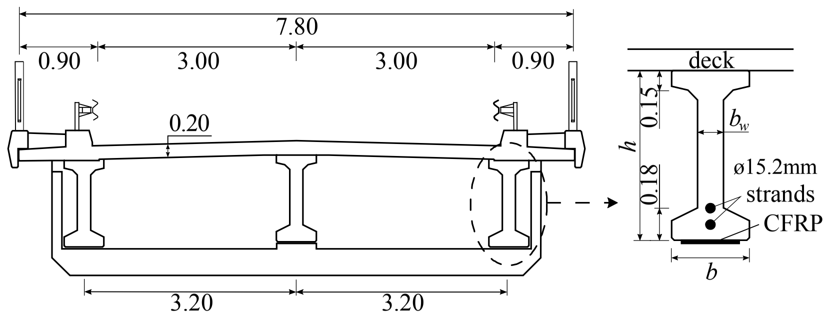

Figure 1. Cross-section and details of the exterior girder (dimensions are in meters if not stated otherwise).

Figure 2

Click here to access/download;Figure;Fig2.pdf

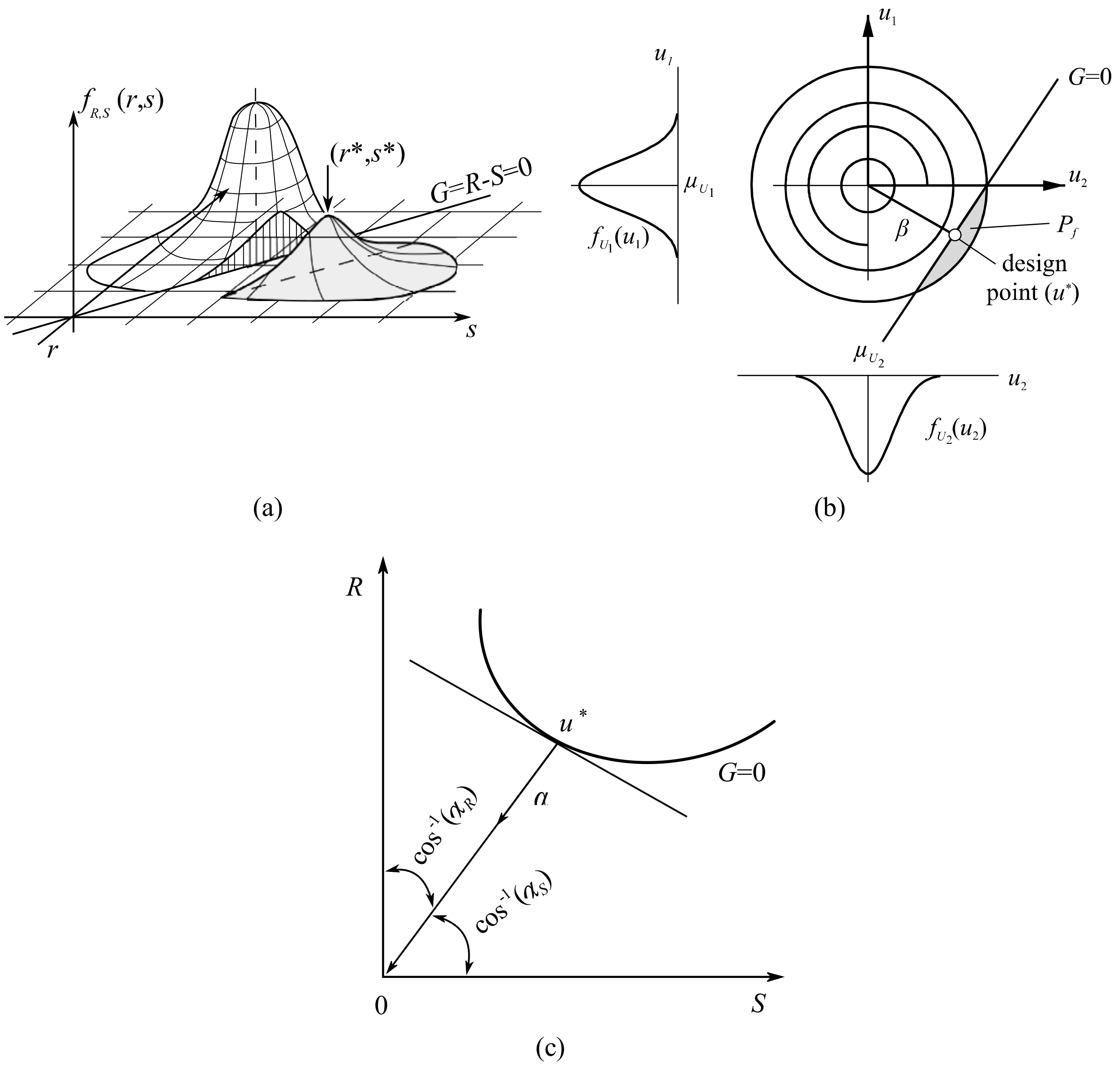

Figure 2. (a) Joint density function $f_{R,S}(r,s)$ of two random variables with marginal density functions f_r and f_s; (b) Reliability index and design point in the standard space, assuming a linear limit state function and two random variables u_1 and u_2; and (c) cosines direction α at design point u^*. Figure adapted from Schneider (1997).

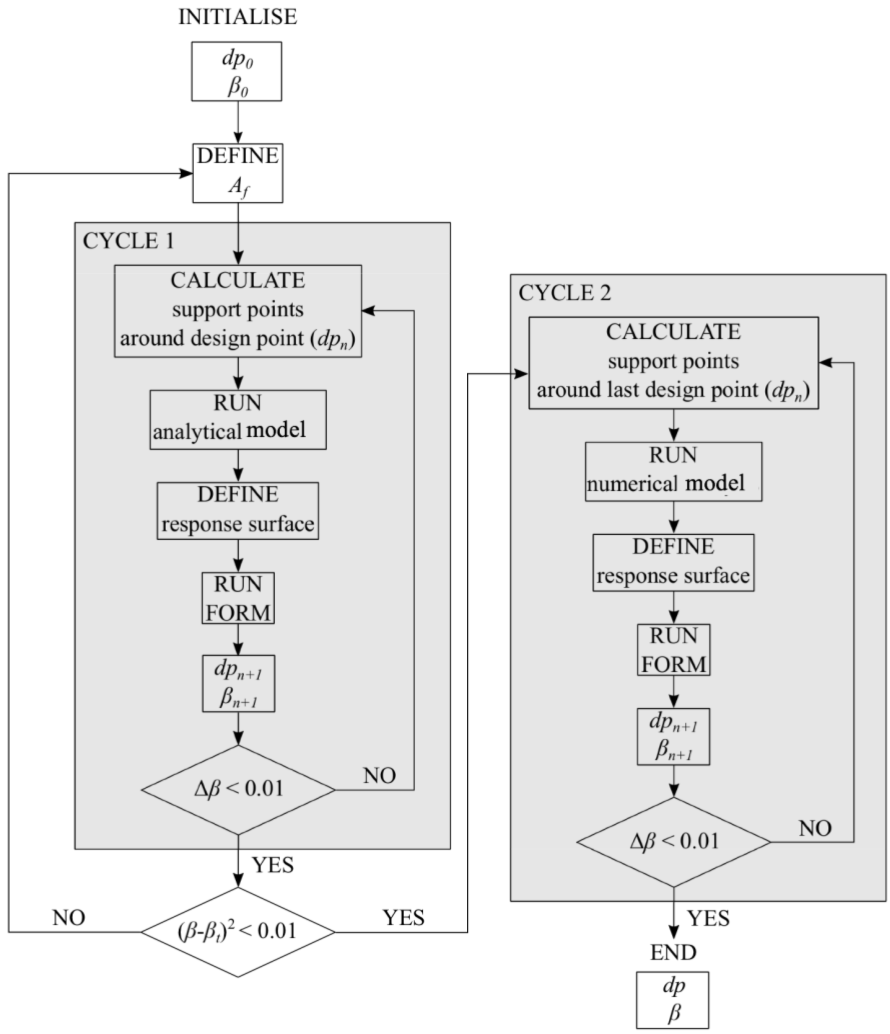

Figure 3. Flowchart showing both stages of analysis and iterative cycles.

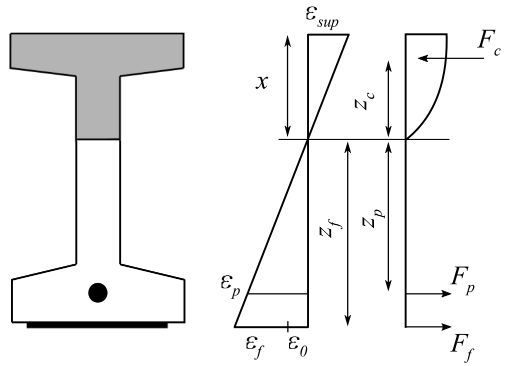

Figure 4. Stress-strain diagram for cross-sectional analysis of PC girders.

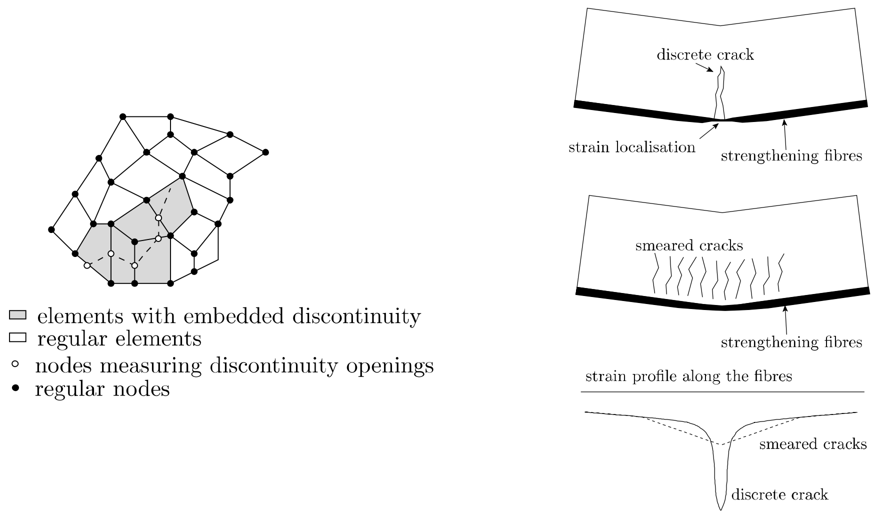

(a) (b)

Figure 5. (a) Finite elements with embedded cracks. (b) Interaction between FRP and cracks in the scope of discrete and smeared models.

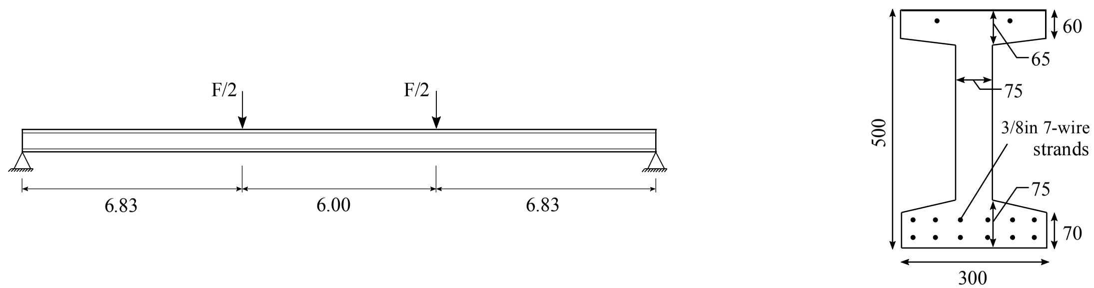

(a) (b)

Figure 6.Loading scheme and cross-section of the girder: (a) side view (dimensions in m); and (b) cross-section (dimensions in mm unless stated otherwise).

(a) (b)

Figure 7. Tested PC girder: (a) control, and (b) CFRP-strengthened girders.

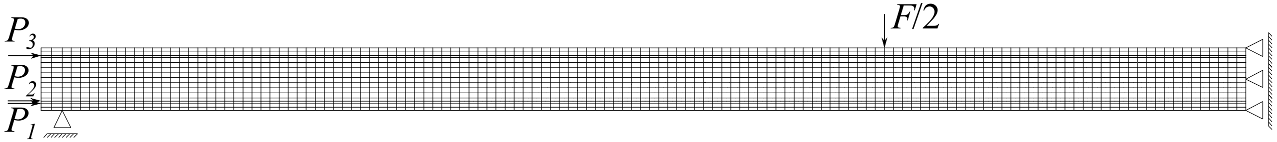

Figure 8. Mesh used in finite element analysis including loading and boundary conditions.

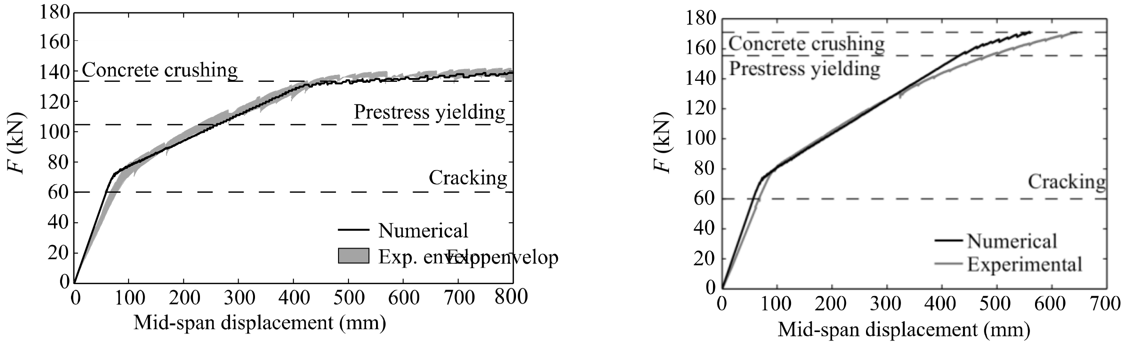

(a) (b)

Figure 9. Load-displacement curves for: (a) non-strengthened; and (b) CFRP-strengthened girders.

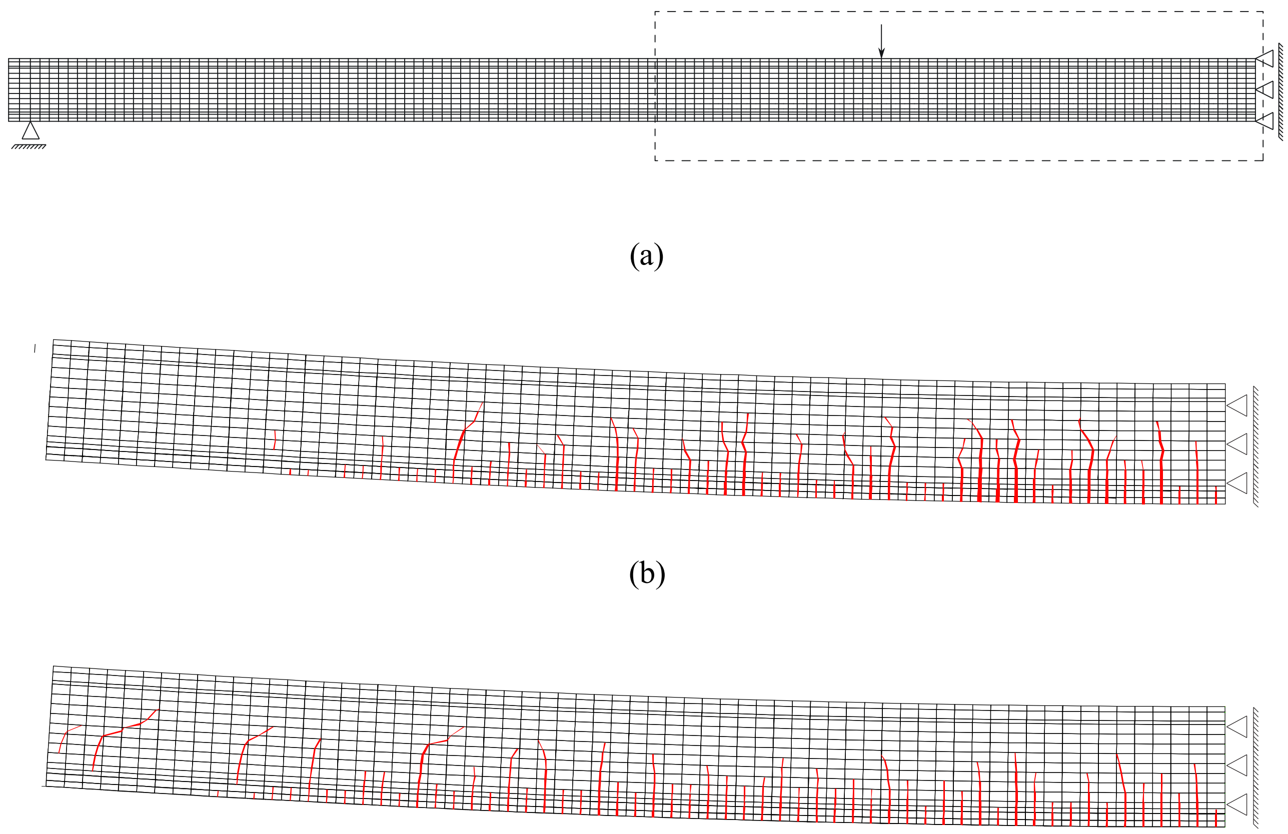

(a)

(b)

(c)

Figure 10. Detail of the deformed shape and crack pattern at failure: (a) identification of the detailed region; (b) non-strengthened; and (c) CFRP-strengthened girders. Note: for illustration purpose crack widths are magnified by a factor of 20 and only widths above 0.25 mm are shown.

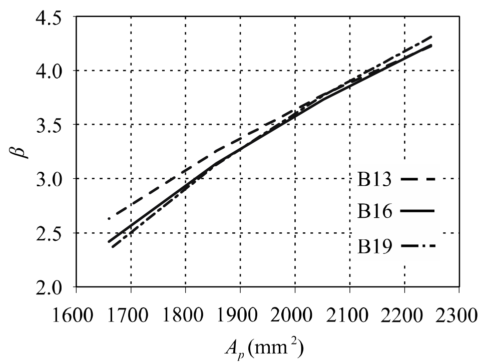

(a)

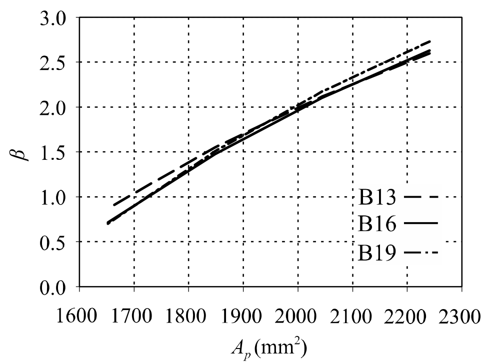

(b)

Figure 11. Reliability index as a function of the area of the pre-tensioning steel in non-strengthened girders according to: (a) RSA (1983); and (b) EN1991-2 (2002)

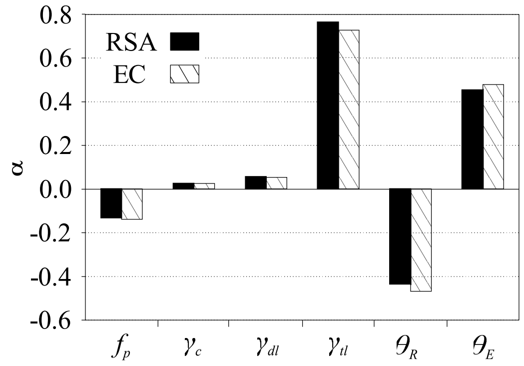

Figure 12. Cosines direction at design point.

Figure 13

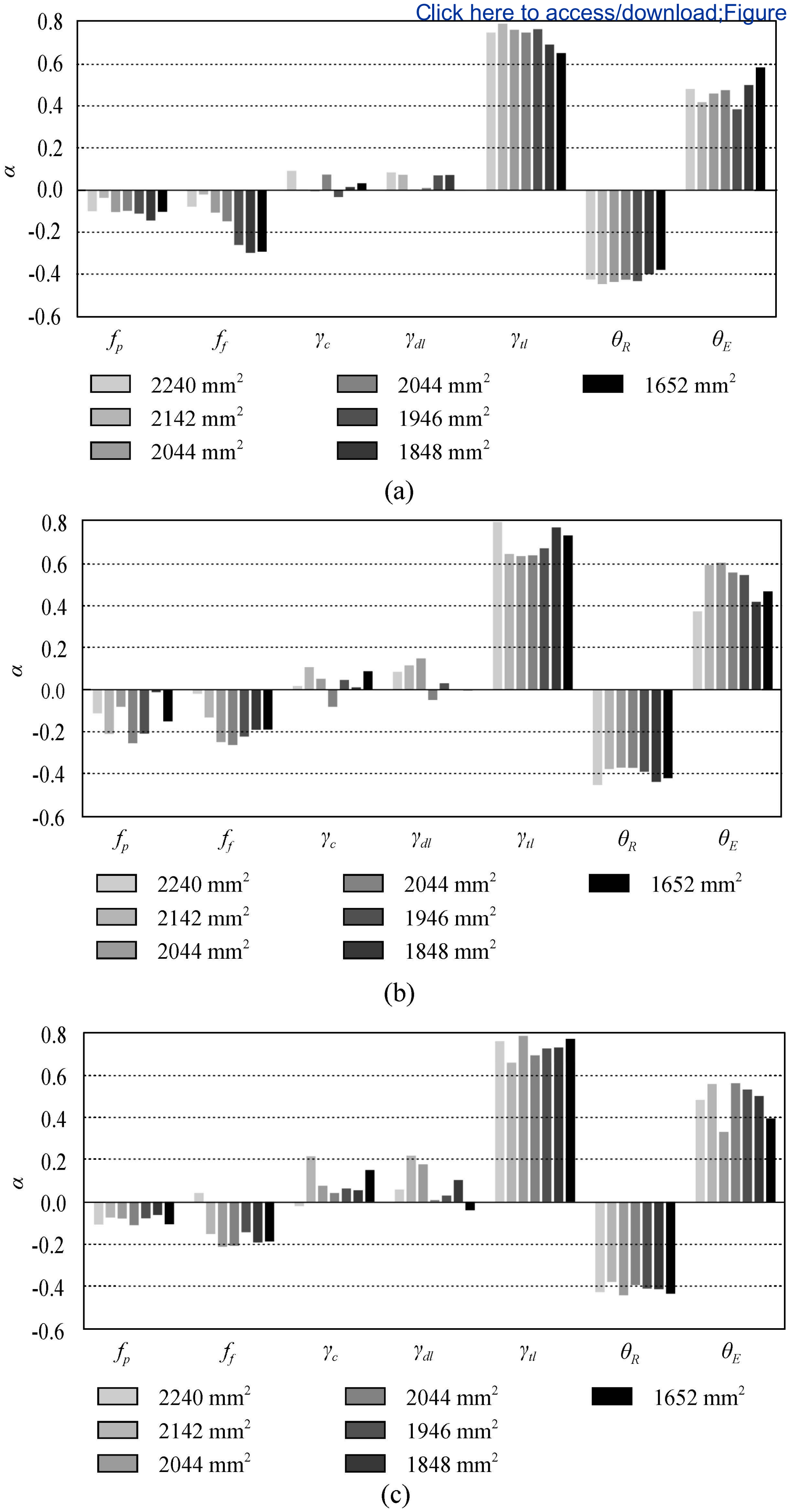

Figure Cosines direction at design point as a function of the pre-tensioning steel (a) B13, (b) B16, and (c) B19.